

Statistical Finite Elements via Langevin Dynamics*

Ömer Deniz Akyildiz^{*,†}, Connor Duffin^{*,‡}, Sotirios Sabanis[§], and Mark Girolami[¶]

Abstract. The recent statistical finite element method (statFEM) provides a coherent statistical framework to synthesise finite element models with observed data. Through embedding uncertainty inside of the governing equations, finite element solutions are updated to give a posterior distribution which quantifies all sources of uncertainty associated with the model. However to incorporate all sources of uncertainty, one must integrate over the uncertainty associated with the model parameters, the known *forward problem* of uncertainty quantification. In this paper, we make use of Langevin dynamics to solve the statFEM forward problem, studying the utility of the unadjusted Langevin algorithm (ULA), a Metropolis-free Markov chain Monte Carlo sampler, to build a sample-based characterisation of this otherwise intractable measure. Due to the structure of the statFEM problem, these methods are able to solve the forward problem without explicit full PDE solves, requiring only sparse matrix-vector products. ULA is also gradient-based, and hence provides a scalable approach up to high degrees-of-freedom. Leveraging the theory behind Langevin-based samplers, we provide theoretical guarantees on sampler performance, demonstrating convergence, for both the prior and posterior, in the Kullback-Leibler divergence, and, in Wasserstein-2, with further results on the effect of preconditioning. Numerical experiments are also provided, for both the prior and posterior, to demonstrate the efficacy of the sampler, with a Python package also included.

Key words. Uncertainty quantification, Finite Element Methods, Inverse Problems, Langevin dynamics

AMS subject classifications. 65C05, 60H15, 65N30, 35R30

1. Introduction. Uncertainty quantification (UQ) is a fundamental aspect of science, with increasing attention being cast upon so-called physics-informed statistical models [3]. Such models recognise the inherent uncertainty in model specification, which will almost certainly lead to misspecification due to incomplete knowledge [22]. A particular approach, named statFEM [20], does so via a probabilistic description of the model variable $u(x)$, $x \in \Omega \subset \mathbb{R}^s$, which for the elliptic PDE case is

$$(1.1) \quad \begin{aligned} \mathcal{L}_\theta u &= f + \xi, \\ \log \theta(x) &\sim \mathcal{GP}(m(x), k_\theta(x, x')), \quad \xi(x) \sim \mathcal{GP}(0, k_\xi(x, x')). \end{aligned}$$

As the mathematical description of the system, this defines the conditional Gaussian process (GP) $p(u | \theta) = \mathcal{GP}([\mathcal{L}_\theta^{-1} f](x), \mathcal{L}_\theta^{-1} k_\xi(x, x') \mathcal{L}_\theta^{-*})$, an infinite-dimensional object. In practice,

*Ö. D. A. was supported by the Lloyd's Register Foundation Data Centric Engineering Programme and EP-SRC Programme Grant EP/R034710/1. C. D and M. G were supported by EPSRC grant EP/T000414/1 and M. G was supported by a Royal Academy of Engineering Research Chair, and EPSRC grants EP/R018413/2, EP/P020720/2, EP/R034710/1, EP/R004889/1. S.S. was supported by the Alan Turing Institute under the EPSRC grant EP/N510129/1.

[†]The Alan Turing Institute, London, NW1 2DB, UK and University of Cambridge, Cambridge, CB2 1PZ, UK

[‡]University of Cambridge, Cambridge, CB2 1PZ, UK

[§]University of Edinburgh, Edinburgh, EH8 9YL, UK and The Alan Turing Institute, London, NW1 2DB, UK

[¶]The Alan Turing Institute, London, NW1 2DB, UK and University of Cambridge, Cambridge, CB2 1PZ, UK

*Corresponding authors: Ö. D. A (odakyildiz@turing.ac.uk) and C. D (cpd32@cam.ac.uk).

discretisation is required, which for finite elements proceeds from the weak form of Equation (1.1),

$$\mathcal{A}_\theta(u, v) = \langle f + \xi, v \rangle, \quad \forall v \in V,$$

where $\mathcal{A}_\theta(\cdot, \cdot)$ is the bilinear form generated from \mathcal{L}_θ , and $\langle \cdot, \cdot \rangle$ is the appropriate Hilbert space inner product. Defining the d -dimensional basis function expansion for $u(x) \approx \sum_{i=1}^d u_i \phi_i(x)$, $v(x) \approx \sum_{i=1}^d v_i \phi_i(x)$ then gives the induced Gaussian

$$p(u | \theta) = \mathcal{N}(A_\theta^{-1}b, A_\theta^{-1}GA_\theta^{-\top}),$$

where $A_{\theta,ij} = \mathcal{A}_\theta(\phi_i, \phi_j)$, $b_j = \langle f, \phi_j \rangle$, $G_{ij} = \langle \phi_i, \langle k_\xi(\cdot, \cdot), \phi_j \rangle \rangle$. The now finite-dimensional probability distribution provides a quantification of the *a priori* belief in the model specification and serves as a reference measure for further inference and data assimilation; observed data, $y \in \mathbb{R}^{d_y}$, can now be incorporated to give the posterior over the FEM coefficients $u \in \mathbb{R}^d$. Examples [13, 14, 17] have demonstrated the usefulness of this approach, with the computed posterior distribution providing a statistically coherent synthesis of physics and data, with an interpretable UQ.

Yet to provide UQ, uncertainty associated with θ must be taken into account in order to compute the statFEM prior and posterior distributions. This requires marginalising over θ ; for the prior this is $p(u) = \int p(u | \theta)p(\theta)d\theta$. This integral is intractable, and some sort of approximation is required. In previous work, θ was either fixed or a first-order expansion was taken, to give an approximate marginal measure. In this work we take a fully Bayesian approach and marginalise over these parameters directly.

Due to stochasticity, a Monte-Carlo (MC) approximation can be used. For elliptic stochastic PDEs, one such approximation is multilevel MC (MLMC) [8, 18], in which the system is solved on a hierarchy of more computationally expensive models, to estimate a possibly nonlinear functional of interest. Additional methods that involve MC sampling for functional estimation are multilevel Markov chain Monte Carlo (MLMCMC) [12] and quasi-MC [21]. However, in this work we target the measure defined by the finite element solution, both *a priori* and *a posteriori*, an inherently high-dimensional probability distribution. Thus in order to estimate $p(u)$ and $p(u | y)$, we require samplers that are robust to mesh-refinement and have been applied to physics-based problems. This has been studied in Bayesian inversion [32].

For high-dimensional sampling in the inverse problems context, Metropolis-Hastings (MH) Markov chain Monte Carlo (MCMC) samplers are often used [29], one example of which is the preconditioned Crank-Nicolson (pCN) algorithm [9]. The pCN algorithm is defined on the function space of the underlying problem, before discretisation, ensuring robustness under mesh-refinement. The standard proposal mechanism uses a random walk, with the covariance being the same as the prior distribution. Extensions of pCN, to alternative proposals that make use of the geometry of the target measure, are also considered in [4, 23]. An alternate approach is the stochastic Newton method [26], which constructs a proposal mechanism from the Hessian of the log-density.

However, in high-dimensional scenarios, recent works have shown that taking an MH-free approach can also lead to efficient samplers that scale well with increasing dimension. Inspired by the success of gradient-based optimisers in machine learning, methods based on Langevin diffusions, such as the unadjusted Langevin algorithm (ULA) [10, 15, 16, 33, 36] have received

significant attention. Our approach is further motivated by the standard ULA iteration, targeting $p(u | \theta)$, being

$$u_k = u_{k-1} - \eta A_\theta^\top G^{-1} (A_\theta u_{k-1} - b) + \sqrt{2\eta} Z_k, \quad Z_k \sim \mathcal{N}(0, I),$$

which does not require the inversion of the FEM stiffness matrix. For judicious choice of the covariance structure of G , this gives an iterative sampling approach which can characterise the measure $p(u | \theta)$ through sparse matrix-vector products, solving the forward problem without ever needing to solve the model itself.

The contribution of this work is to establish a link between popular gradient-based sampling methods and statFEM, paving the way for their general use in stochastic elliptic PDEs. These schemes are based on Euler discretisations of continuous-time Langevin diffusions, and, due to the structure of statFEM, assumptions required for these algorithms to perform well are satisfied a priori: they are ideal tools to sample the induced measures. After defining the problem in Section 2, we define various samplers and provide explicit convergence rates in both the KL divergence and in Wasserstein-2, for both the prior and posterior measures, in Section 3. We also study the effect of preconditioning on the allowed step-sizes of the algorithm. In Section 4, we empirically demonstrate these results on case studies for the Poisson equation both *a priori* and *a posteriori*. We also include a Python package to accompany this paper, containing all implementations*.

This paper enables the use of similar samplers in this framework, such as variance-reduced, underdamped, decentralised, and parallelised Langevin algorithms. All of these schemes can be analysed and incorporated by extending the techniques we provide in this paper and can contribute to the use of the statFEM methodology under various scenarios where other samplers may be preferable.

Notation. For a set A , we denote its boundary as ∂A . We denote the space of functions which are compactly supported and infinitely differentiable with \mathcal{C}_c^∞ . We say that $v : \Omega \rightarrow \mathbb{R}$ is a weak derivative of $u : \Omega \rightarrow \mathbb{R}$ in the direction of the i th coordinate if

$$\int_{\Omega} u(x) \varphi(x) dx = - \int_{\Omega} v(x) \frac{\partial \varphi}{\partial x_i}(x) dx,$$

for all compactly supported functions $\varphi \in \mathcal{C}_c^\infty$. The Sobolev space $H^1(\Omega)$ is defined as a set of all functions that are square integrable and have weak derivatives in all coordinate directions. We also define the Sobolev space $H_0^1(\Omega)$ to denote the functions $u \in H^1(\Omega)$ and identically zero on $\partial\Omega$. The notation $L^2(\Omega)$ denotes the space of square-integrable functions and $\langle f, g \rangle = \int_{\Omega} f(x)g(x)dx$ the associated inner product w.r.t. the Lebesgue measure.

2. Statistical Finite Elements for Linear PDEs. Consider the elliptic example of Section 1, Equation (1.1), with Dirichlet boundary conditions

$$(2.1) \quad \begin{aligned} \mathcal{L}_\theta u &= f + \xi, & x \in \Omega, \\ u &= 0, & x \in \partial\Omega, \end{aligned}$$

*Available at <https://www.github.com/connor-duffin/ula-statfem>

where $u := u(x)$, $f = f(x)$, $x \in \Omega \subset \mathbb{R}^d$. We note that hyperparameters of the Gaussian processes ξ , θ are assumed to be known.

A Gaussian prior measure can be constructed by considering the weak solutions of (2.1), conditioned on θ . The weak form is specified from multiplying both sides of the equation with a test function $v \in H_0^1(\Omega)$, assuming that $u \in H_0^1(\Omega)$, $f, \xi \in L^2(\Omega)$, and $\theta \in L^\infty(\Omega)$, and integrating over Ω ,

$$(2.2) \quad \mathcal{A}_\theta(u, \psi) = \langle f, \psi \rangle + \langle \xi, \psi \rangle.$$

The space $H_0^1(\Omega)$ admits an orthonormal basis $\{\phi_i\}_{i \in \mathbb{N}}$, so for $u \in H_0^1(\Omega)$, $u = \sum_{i=1}^{\infty} u_i \phi_i(x)$ and hence

$$\sum_{i=1}^{\infty} u_i \mathcal{A}_\theta(\phi_i, \phi_j) = \langle f, \phi_j \rangle + \langle \xi, \phi_j \rangle, \quad j \in \mathbb{N},$$

as $v \in H_0^1(\Omega)$. Therefore, \mathcal{A}_θ can be seen as an infinite dimensional matrix A_θ with entries $A_{\theta,ij} = \mathcal{A}_\theta(\phi_i, \phi_j)$.

To construct the finite-dimensional approximation, we first subdivide the domain Ω to construct the triangulation $\Omega_h \subset \Omega$, with vertices $\{x_j\}_{j=1}^d$, where the maximal length of the sides of the triangulation is given by h . The polynomial basis functions $\{\phi_j\}_{j=1}^d$ are then defined on the mesh, having the property that $\phi_i(x_j) = \delta_{ij}$. In this work we consider the linear polynomial $C^1(\Omega)$ basis functions only, and denote by $V_h \subset H_0^1(\Omega)$ as the span of these basis functions. Projecting from the infinite-dimensional space gives the finite-dimensional approximation $u(x) \approx u_h(x) = \sum_{j=1}^d u^{(j)} \phi_j(x)$. The vector of FEM coefficients is $u = (u^{(1)}, \dots, u^{(d)})$, reusing the notation from (2.1); dimensionality should be clear from context.

The finite-dimensional weak form induces a Gaussian distribution over the FEM coefficients u . Conditioned on θ , this is

$$(2.3) \quad p(u|\theta) = \mathcal{N}(A_\theta^{-1}b, A_\theta^{-1}GA_\theta^{-\top}),$$

where $A_{\theta,ij} = \mathcal{A}_\theta(\phi_i, \phi_j)$, $b_j = \langle f, \phi_j \rangle$, and $G_{ij} = \langle \phi_i, \langle k_\xi(\cdot, \cdot), \phi_j \rangle \rangle$. The marginal distribution of the solution u is

$$(2.4) \quad p(u) = \int p(u|\theta)p(\theta)d\theta,$$

and the first goal in this paper is to describe a methodology for sampling from this marginal. This is done in Section 2.2, by targeting the joint $p(u, \theta) = p(u|\theta)p(\theta)$ and considering the marginal of u . Our second goal is to sample from the posterior distribution

$$(2.5) \quad p(u|y) = \frac{p(u, y)}{p(y)}$$

To solve this problem, we construct samplers in the extended space $p(u, \theta|y)$ and target its u -marginal. The inference of the solution amounts to a Bayesian inference procedure and we tackle this problem by developing a sampler for the posterior measure over the numerical solutions of the PDE under consideration, in Section 2.3.

We note that a classical approach to sample from the joint $p(u, \theta)$ is to consider a Gibbs sampler which targets $p(u | \theta)$ and $p(\theta | u)$ in turn. However, as $p(\theta | u)$ is not of the form of any known distribution (whilst its prior is a GP), we choose to sample from the marginal through exact sampling from $p(\theta)$, which can be done efficiently using, for example, Kronecker methods [31] or circulant embedding [11]. We also note that this approach is useful in scenarios in which samples from θ have already been obtained, from some distribution of interest, and their effect on the model solutions is desired.

2.1. Conditional Langevin SDEs. In this section, we introduce conditional Langevin SDEs to sample from $p(u|\theta)$ and $p(u|y, \theta)$ for fixed θ . In particular, we consider

$$(2.6) \quad du_t = -\nabla\Phi_\theta(u_t)dt + \sqrt{2}dB_t,$$

where $(B_t)_{t \geq 0}$ is a Brownian motion and

$$\Phi_\theta(u) = \frac{1}{2}(A_\theta u - b)^\top G^{-1}(A_\theta u - b).$$

By construction, this SDE targets the conditional distribution given in Eq. (2.3). The potential advantage of using such a diffusion can already be observed by the expression of the diffusion given in (2.6). In particular, note that the drift in this diffusion is given by

$$(2.7) \quad \nabla_u \Phi_\theta(u) = A_\theta^\top G^{-1} A_\theta u - A_\theta^\top G^{-1} b.$$

This expression does not contain any inverse of the form A_θ^{-1} which implies an efficient computational scheme. Note that here G^{-1} is a matrix that is easy to invert, e.g., a diagonal matrix.

Before going into an efficient discretisation of the conditional Langevin diffusion, we note that the SDE in (2.6) has an analytical solution as summarised in the following remark.

Remark 2.1. The Langevin SDE given in (2.6) has the following analytical solution (see, e.g., [36])

$$(2.8) \quad u_t \stackrel{d}{=} A_\theta^{-1} b + e^{-tA_\theta^\top G^{-1} A_\theta} (u_0 - A_\theta^{-1} b) + (A_\theta^{-1} G A_\theta^{-\top})^{1/2} \left(I - e^{-2tA_\theta^\top G^{-1} A_\theta} \right)^{1/2} Z$$

where $Z \sim \mathcal{N}(0, I)$ is independent of u_0 .

It is clear that having an analytical solution is not useful in this example, since it necessitates computing A_θ^{-1} and other extra computations, which ends up being impractical compared to performing an inversion in the first place. However, despite the exact solution requiring heavy computations, the associated numerical scheme to the Langevin SDE does not require the same computational resources, and can be formally shown to track the underlying diffusion closely.

To sample from the conditional SDE targeting $p(u|\theta) \propto \exp(-\Phi_\theta(u))$, we consider the unadjusted Langevin algorithm (ULA) which is the standard Euler-Maruyama discretisation of the SDE (2.6) and given as

$$(2.9) \quad \begin{aligned} u_{k+1} &= u_k - \eta \nabla_u \Phi_\theta(u_k) + \sqrt{2\eta} Z_{k+1}, \\ &= u_k - \eta A_\theta^\top G^{-1} A_\theta u_k + \eta A_\theta^\top G^{-1} b + \sqrt{2\eta} Z_{k+1}, \end{aligned}$$

where $(Z_k)_{k \geq 0}$ are i.i.d standard Normal random variables, $Z_k \sim \mathcal{N}(0, I)$ for every k . Given that this scheme consists of a noisy linear mapping, we can also write down the asymptotic distribution of the ULA exactly. To see this, first rewrite the iterations as

$$u_{k+1} - A_\theta^{-1}b = (I - \eta A_\theta^\top G^{-1} A_\theta)(u_k - A_\theta^{-1}b) + \sqrt{2\eta}Z_{k+1}.$$

then limiting distribution of the conditional ULA is [36]

$$p_\infty^\eta = \mathcal{N}\left(A_\theta^{-1}b, A_\theta^{-1}G A_\theta^{-\top} \left(I - \frac{\eta}{2} A_\theta^\top G^{-1} A_\theta\right)^{-1}\right).$$

It is interesting to observe that, in this case, the mean estimates computed using the stationary measure would be unbiased. The discretisation scheme results in the bias of the uncertainty estimates, which can be made arbitrarily small as $\eta \rightarrow 0$.

To sample from the conditional posterior distribution $p(u|y, \theta)$, we define the potential

$$\begin{aligned} \Phi_\theta^y(u) &= -\log p(u|y, \theta) \\ &= -\log p(y|u) - \log p(u|\theta). \end{aligned}$$

In this case, the Langevin SDE targeting $p(u|y, \theta)$ takes the form

$$u_{k+1} = u_k - \eta \nabla_u \Phi_\theta^y(u_k) + \sqrt{2\eta}Z_{k+1}.$$

Note that this scheme is general and can handle nonlinear observation models unlike an exact sampling method.

2.2. Unadjusted Langevin algorithm for sampling the prior measure. The first problem we are interested in solving is to sample from the marginal prior of the solutions $p(u)$ induced by the statistical FEM construction. To solve this problem, we design a sampler that targets the joint distribution $p(u, \theta)$ and we obtain the marginal $p(u)$ from these samples. In order to sample from the joint $p(u, \theta)$, we leverage the conditional schemes and consider the following scheme

$$(2.10) \quad \theta \sim p(\theta),$$

$$(2.11) \quad u_{k+1} = u_k - \eta \nabla_u \Phi_\theta(u_k) + \sqrt{2\eta}Z_{k+1}.$$

We show in Sec. 3 that this scheme can indeed be used for approximately sampling from the marginal prior $p(u)$ and provide some theoretical guarantees for this sampler.

2.3. Unadjusted Langevin algorithm for sampling the posterior measure. Sampling from $p(u)$ is not our final goal, as we are interested in sampling from the posterior measure $p(u|y)$. To this end, we consider the sampler

$$(2.12) \quad \theta \sim p(\theta),$$

$$(2.13) \quad u_{k+1} = u_k - \eta \nabla_u \Phi_\theta^y(u_k) + \sqrt{2\eta}Z_{k+1}.$$

which samples from $p(u, \theta|y)$ (See Section 3). We note that

$$\nabla \Phi_\theta^y(u) = -\nabla \log p(u|y, \theta) = -\nabla \log p(y|u) - \nabla \log p(u|\theta).$$

Therefore the implementation of the recursions (2.12)–(2.13) are straightforward given θ .

2.4. Preconditioned unadjusted Langevin schemes. For badly conditioned problems, preconditioning can improve the convergence and stability of the above ULA schemes significantly. Therefore, to sample from the prior measure $p(u)$, we consider the preconditioned sampler

$$(2.14) \quad \theta \sim p(\theta)$$

$$(2.15) \quad u_{k+1} = u_k - \eta M \nabla \Phi(u_k) + \sqrt{2\eta} M^{1/2} W_{k+1},$$

where $(W_k)_{k \geq 0}$ is the sequence of standard Normal random variables. Similarly, in order to sample from the posterior $p(u|y)$, we consider

$$(2.16) \quad \theta \sim p(\theta)$$

$$(2.17) \quad u_{k+1} = u_k - \eta M \nabla \Phi_\theta^y(u_k) + \sqrt{2\eta} M^{1/2} W_{k+1}.$$

We provide theoretical analysis of the preconditioned schemes in Section 3.4 and demonstrate their utility in Section 4.

2.5. The Algorithm. To draw an approximate sample from the marginal distributions $p(u)$ or $p(u|y)$, using ULA, the approach we take in this paper is to first draw $\theta_k \sim p(\theta)$, and then run a sub-chain for $p(u|\theta_k)$ (or $p(u|\theta_k, y)$), for n_{inner} iterations. This sub-chain is initialised to the previous iterate u_{k-1} . Due to the warm start, it is assumed that n_{inner} is small; in Section 4 we take $n_{\text{inner}} = O(10)$. Note also that the inner iterations are cheap as there is no requirement for FEM assembly, requiring only matrix-vector products with the sparse A_θ . This gives the set of samples $\{u_{i,k}\}_{i=1}^{n_{\text{inner}}} \sim p(u|\theta_k)$, and we take the joint sample as $(u_k, \theta_k) = (u_{n_{\text{inner}},k}, \theta_k) \sim p(u, \theta)$ (the full algorithm is shown in Algorithm 2.1). The inner iterations ensure that the sample is taken from the target measure, whilst also decorrelating the u_k samples.

Algorithm 2.1 StatFEM ULA sampler.

Let $M \in \mathbb{R}^{d \times d}$ be the preconditioner, $u_0 \in \mathbb{R}^d$ the initial condition.

for $k = 1, \dots, K$ **do**

$\theta_k \sim p(\theta)$.

$u_{0,k} = u_{k-1}$.

for $i = 1, \dots, n_{\text{inner}}$ **do**

$Z_{i,k} \sim \mathcal{N}(0, I)$.

$u_{i,k} = u_{i-1,k} - \eta M \nabla \Phi_\theta(u_{i-1,k}) + \sqrt{2\eta} M^{1/2} Z_{i,k}$

end for

$u_k = u_{n_{\text{inner}},k}$.

end for

return $\{(u_k, \theta_k)\}_{k=1}^K$

3. Analysis. In this section, we analyse the proposed schemes and prove convergence rates. In particular, in Section 3.1, we prove the convergence of the conditional ULA chains, where the $(u_k)_{k \geq 0}$ iterates run with fixed θ . Then, in Section 3.2, we start by analysing the sampler defined in Eqs. (2.10)–(2.11). This sampler aims at sampling from the marginal $p(u)$. Next, in

Section 3.3, we analyse the sampler defined in Eqs. (2.12)–(2.13). This analysis follows from similar arguments of the analysis of the marginal sampler of $p(u)$. Finally, in Section 3.4, we extend these results to the case when the preconditioners are used in the ULA chains. We demonstrate, quantitatively, that a good preconditioner choice can impact and improve the error and convergence rates significantly, an observation we verify in the experimental section.

Throughout this section, we assume the following.

Assumption 1. *We assume there exists $m > 0$ and $L > 0$ such that*

$$(3.1) \quad 0 < m = \inf_{\theta} \lambda_{\min}(A_{\theta}^{\top} G^{-1} A_{\theta}) \quad \text{and} \quad L = \sup_{\theta} \lambda_{\max}(A_{\theta}^{\top} G^{-1} A_{\theta}) < \infty.$$

This assumption implies that, for every θ , we have

$$mI \preceq \nabla^2 \Phi_{\theta}(u) \preceq LI.$$

Using this definition, we also define *the worst-case condition number*

$$(3.2) \quad \kappa_{\max} := \frac{L}{m} < \infty.$$

The existence and finiteness of these quantities is verifiable under some conditions.

3.1. The analysis in KL divergence for the conditional ULA. Two standard conditions for analysing the convergence of Langevin-type scheme is strong convexity and gradients of the potential being Lipschitz. In our case, we can prove that these conditions hold as follows.

Lemma 3.1. *Given Assumption 1, the gradient $\nabla \Phi_{\theta}(u)$ is Lipschitz, i.e.,*

$$\|\nabla \Phi_{\theta}(u) - \nabla \Phi_{\theta}(u')\| \leq L_{\theta} \|u - u'\|,$$

where $L_{\theta} = \lambda_{\max}(A_{\theta}^{\top} G^{-1} A_{\theta})$. Moreover, for fixed θ , the function $\Phi_{\theta}(\cdot)$ is strongly convex with $m_{\theta} = \lambda_{\min}(A_{\theta}^{\top} G^{-1} A_{\theta}) > 0$ which follows from Assumption 1.

Proof. The first claim follows from

$$\begin{aligned} \|\nabla_u \Phi_{\theta}(u) - \nabla_u \Phi_{\theta}(u')\| &= \|A_{\theta}^{\top} G^{-1} A_{\theta} u - A_{\theta}^{\top} G^{-1} A_{\theta} u'\|, \\ &\leq L_{\theta} \|u - u'\|, \end{aligned}$$

where the last line is obtained by the properties of the matrix norm. For proving the second claim, note that a function is strongly convex iff $\nabla^2 \Phi_{\theta}(u) \succeq m_{\theta} I$. In our case, $\nabla^2 \Phi_{\theta}(u) = A_{\theta}^{\top} G^{-1} A_{\theta}$, hence $m_{\theta} = \lambda_{\min}(A_{\theta}^{\top} G^{-1} A_{\theta}) > 0$. ■

Assumption 1 states that $L = \sup_{\theta} L_{\theta} < \infty$ and $m = \inf_{\theta} m_{\theta} > 0$.

Next, we provide the convergence rate of the conditional ULA, adapted from [33].

Theorem 3.2. *Under Assumption 1 and step-size given by $0 < \eta \leq \frac{m_{\theta}}{4L_{\theta}^2}$, we have*

$$\text{KL}(p_k(u|\theta) \| p(u|\theta)) \leq e^{-m_{\theta} \eta k} \text{KL}(p_0(u) \| p(u|\theta)) + 8\eta d L_{\theta} \kappa_{\theta},$$

where κ_{θ} is the condition number of the matrix $A_{\theta}^{\top} G^{-1} A_{\theta}$.

Proof. Using Theorem 2 in [33], we directly obtain

$$\text{KL}(p_k(u|\theta), p(u|\theta)) \leq e^{-m\eta k} \text{KL}(p_0(u), p(u|\theta)) + \frac{8\eta d L_\theta^2}{m_\theta}.$$

Observing that $\kappa_\theta = L_\theta/m_\theta$ is the condition number of the matrix $A_\theta^\top G^{-1} A_\theta$, we obtain the result. \blacksquare

This result is for fixed θ , but still is insightful to demonstrate the dependence of the error bound to the condition number of the matrix $A_\theta^\top G^{-1} A_\theta$. This bound readily implies that we have to choose small step-sizes for badly conditioned problems. Furthermore, it also motivates preconditioning to improve this condition number, as we will discuss in Sec. 3.4.

3.2. The analysis in KL divergence for the ULA prior sampler. In this section, we prove theoretical guarantees for the sampler defined in (2.10)–(2.11).

Similarly to the conditional case, we can still attain a similar result for the marginal sampler of u as the conditional case as we outline below.

Theorem 3.3. *Under Assumption 1 and $0 < \eta \leq \frac{m}{4L^2}$,*

$$\text{KL}(p_k(u)||p(u)) \leq e^{-m\eta k} \mathbb{E}[\text{KL}(p_0(u)||p(u|\theta))] + 8\eta L d \kappa_{\max},$$

where κ_{\max} is given in (3.2).

Proof. This result is a straightforward consequence of Thm. 3.2. In particular, taking expectations of the bound provided in Thm. 3.2 w.r.t. θ , we obtain for the l.h.s.

$$\begin{aligned} \int \text{KL}(p_k(u|\theta)||p(u|\theta))p(\theta)d\theta &= \int \int \log \frac{p_k(u|\theta)}{p(u|\theta)} p_k(u|\theta)p(\theta)dud\theta, \\ &= \int \int \log \frac{p_k(u|\theta)p(\theta)}{p(u|\theta)p(\theta)} p_k(u|\theta)p(\theta)dud\theta, \\ &= \text{KL}(p_k(u, \theta)||p(u, \theta)). \end{aligned}$$

Then, Thm. 3.2 implies that

$$\text{KL}(p_k(u, \theta)||p(u, \theta)) \leq e^{-m\eta k} \mathbb{E}[\text{KL}(p_0(u)||p(u|\theta))] + 8\eta L d \kappa_{\max},$$

by observing that $L_\theta < L$ and $m < m_\theta$ for every θ and $\kappa_{\max} = L/m$. Finally the chain rule of KL-divergence (see Lemma A.1) implies that

$$\text{KL}(p_k(u)||p(u)) \leq \text{KL}(p_k(u, \theta)||p(u, \theta)),$$

which concludes the proof. \blacksquare

These guarantees, based on the KL divergence, can be extended to the Wasserstein-2 distance. This is summarised in the following proposition.

Proposition 3.4. *Let Assumption 1 hold and $\eta \leq 2/(m + L)$. Then, we can obtain*

$$(3.3) \quad W_2(p_k(u), p(u)) \leq \sqrt{2}(1 - m\eta)^k \mathbb{E}[W_2(p_0(u), p(u|\theta))] + \frac{7}{3}\kappa(\eta d)^{1/2}.$$

Proof. Note that, we can write for $\eta \leq 2/(m + L)$ that

$$W_2^2(p_k(u|\theta), p(u|\theta)) \leq 2(1 - m\eta)^{2k} W_2^2(p_0(u), p(u|\theta)) + \frac{49}{9} \kappa^2 \eta d$$

as a consequence of Theorem 1 in [10] and $(a + b)^2 \leq 2a^2 + 2b^2$. Now using Lemma A.2, we can obtain

$$W_2^2(p_k(u), p(u)) \leq 2(1 - m\eta)^{2k} \mathbb{E}[W_2^2(p_0(u), p(u|\theta))] + \frac{49}{9} \kappa^2 \eta d.$$

Using $\sqrt{x + y} \leq \sqrt{x} + \sqrt{y}$ and the Jensen's inequality, we obtain the claimed result. \blacksquare

A similar result was provided for mixtures of log-concave distributions in [10, Theorem 3].

3.3. The analysis in KL divergence for the ULA sampler for the posterior. In this section, we analyse the sampler (2.12)–(2.13). We first note that the distribution $p(y|u)$ denotes observation model. Next, in order to define the sampler, we define the potential

$$(3.4) \quad \Phi_\theta^y(u) = -\log p(y|u) - \log p(u|\theta).$$

Note that, we allow here for general observation models $p(y|u)$ which can be potentially nonlinear. Then we assume the following lower and upper bounds.

Assumption 2. We assume there exists $m_y > 0$ and $L_y > 0$ such that

$$(3.5) \quad 0 < m_y = \inf_{\theta, u} \lambda_{\min}(\nabla^2 \Phi_\theta^y(u)) \quad \text{and} \quad L_y = \sup_{\theta, u} \lambda_{\max}(\nabla^2 \Phi_\theta^y(u)) < \infty.$$

In other words,

$$m_y I \preceq \nabla^2 \Phi_\theta^y(u) \preceq L_y I.$$

for every $u \in \mathbb{R}^d$.

Similar to the previous section, we define the worst-case condition number related to the posterior as

$$(3.6) \quad \kappa_{\max}^y = \frac{L_y}{m_y}.$$

Remark 3.5. (Non-log-concave likelihoods) Recall that

$$\Phi_\theta^y(u) = \Phi_\theta(u) - \log p(y|u).$$

Since we know that Φ_θ already satisfies Assumption 1, this allows for $\log p(y|u)$ to be non-log-concave, as long as Φ_θ^y is still strongly convex. In other words, if the problem is well-conditioned, we can handle non-log-concave nonlinear observation models. In particular, if $\Phi_\theta(u)$ is m -strongly convex, then we can afford $-\log p(y|u)$ to be $(m - m_y)$ -weakly-convex (for $m_y < m$)

in the sense of [34][†] so that $\Phi_\theta^y(u)$ is m_y -strongly-convex. Note that, this also demonstrates that the lack of strong log-concavity of $p(y|u)$ results in a slower convergence rate and a worse condition number.

Remark 3.6. (Non-log-concave likelihoods II) We further note that all results we have derived hold under a more general assumption on target distributions, namely the Log-Sobolev inequality (LSI) [33] (which includes a family of non-log-concave likelihoods). This implies that, given that $\Phi_\theta(u)$ is strongly-convex, this allows $-\log p(y|u)$ to be non-convex (even weaker than weak-convexity), as long as the posterior $p(u|y)$ satisfies the LSI. This may account for a large family of likelihoods in practice.

In the linear case, following [20], we define the observation model as

$$(3.7) \quad y = Hu + e,$$

where Hu is the projected finite element solution and $e \sim \mathcal{N}(0, R)$. We assume that e is a d_y -dimensional zero-mean Gaussian random variable with covariance $R = \sigma_e^2 I$. Therefore the conditional $p(y|u)$ can be written explicitly as

$$(3.8) \quad p(y|u) = \mathcal{N}(Hu, R).$$

In this case, we obtain

$$(3.9) \quad \Phi_\theta^y(u) = -\log \mathcal{N}(y; Hu, R) - \log \mathcal{N}(u; A_\theta^{-1}b, A_\theta^{-\top}GA_\theta^{-1}).$$

We then have

$$\begin{aligned} \nabla_u \Phi_\theta^y(u) &= -H^\top R^{-1}(y - Hu) + A_\theta^\top G^{-1}A_\theta u - A_\theta^\top G^{-1}b, \\ &= (A_\theta^\top G^{-1}A_\theta + H^\top R^{-1}H)u - H^\top R^{-1}y - A_\theta^\top G^{-1}b. \end{aligned}$$

Note that

$$\nabla^2 \Phi_\theta^y(u) = A_\theta^\top G^{-1}A_\theta + H^\top R^{-1}H.$$

The meaning of Assumption 2 in this case is that the contribution from the matrix $H^\top R^{-1}H$ should not make the condition number worse. In this case, it can be verified that this term has positive eigenvalues, therefore Assumption 2 holds in practical settings. This assumption in particular implies that Φ_θ^y is L_y -smooth and m_y -strongly convex.

Next, we state our result.

Theorem 3.7. *Let Assumption 2 hold and $0 < \eta \leq \frac{m_y}{L_y^2}$. Then, we have*

$$\text{KL}(p_k(u|\theta, y) || p(u|\theta, y)) \leq e^{-m_y \eta k} \text{KL}(p_0(u) || p(u|y, \theta)) + 8\eta d L_y \kappa_{\max}^y.$$

[†]A function $f(x)$ is ρ -weakly-convex if

$$f(x) + \frac{s}{2} \|x\|_2^2$$

is convex for $s \geq \rho$.

Proof. The proof is identical to the proof of Theorem 3.2 since $p(\cdot|\theta, y)$ is m^y -log-strongly concave and L^y log-smooth. ■

A similar argument as in the previous section lets us to obtain our final result about the posterior measure $p(u|y)$.

Theorem 3.8. *Under Assumption 2 and $0 < \eta \leq \frac{m_y}{4L_y^2}$,*

$$\text{KL}(p_k(u|y)||p(u|y)) \leq e^{-m_y \eta^k} \mathbb{E} [\text{KL}(p_0(u)||p(u|\theta, y))] + 8\eta L_y d\kappa_{\max}^y,$$

where κ_{\max}^y is given in (3.6).

Proof. The proof is straightforward and follows the same steps as Theorem 3.3 by replacing the notation for the prior with the posterior. ■

3.4. The analysis of the preconditioned Langevin schemes. To improve convergence, we also consider the preconditioned ULA. We start with the conditional case, targeting $p(u|\theta)$, whose Langevin diffusion has the form

$$(3.10) \quad du_t = -M \nabla \Phi_\theta(u_t) dt + \sqrt{2} M^{1/2} dB_t.$$

The strategy used in this part of the analysis is to rewrite this diffusion as a standard overdamped diffusion with a variable transformation (see, e.g., [2]). This allows us to utilise the results for the standard conditional diffusion and obtaining the same rates by using the fact that the KL divergence is invariant w.r.t. invertible transformations. Given the convergence results of the conditional case, it is straightforward to extend our results for the marginal sampler defined in (2.14)–(2.15) and the posterior sampler defined in (2.16)–(2.17), as we demonstrate below.

To show that the diffusion defined in (3.10) would still target the right stationary measure, we define the following variable [2]

$$z = M^{-1/2} u.$$

By applying Ito's formula, we obtain

$$(3.11) \quad dZ_t = -\nabla_z \Phi_\theta^M(Z_t) dt + \sqrt{2} dB_t,$$

where $\Phi_\theta^M(\cdot) = \Phi_\theta \circ M^{1/2}(\cdot)$. It is easy to see that, given $\Phi_\theta^M(z) = \Phi_\theta(M^{1/2}z)$, we can write

$$\nabla_z \Phi_\theta^M(z(u)) = D(u(z)) \nabla_u \Phi_\theta(u)$$

where $D(u(z)) = M^{\top/2}$ is the Jacobian of the transformation.

It can be also seen that the stationary measure of (3.11)

$$p_\infty(z) \propto \exp(-\Phi_\theta^M(z)),$$

and the standard transformation of the random variables implies that this leaves the original stationary measure invariant, i.e., $p_\infty(u) \propto \exp(-\Phi_\theta(u))$ since M is independent of u , the determinant term cancels.

It is easy to see that the convergence rate of the diffusion (3.11) would be determined by the properties of the new map Φ_θ^M for fixed θ . Therefore, we first remark the properties of this map. In order to first analyse the sampler (2.14)–(2.15), we first start with a lemma which follows from Assumption 1.

Lemma 3.9. *There exists $m_M > 0$ and $L_M > 0$ such that*

$$(3.12) \quad 0 < m_M = \inf_{\theta} \lambda_{\min}(M^{\top/2} A_{\theta}^{\top} G^{-1} A_{\theta} M^{1/2})$$

and

$$(3.13) \quad L_M = \sup_{\theta} \lambda_{\max}(M^{\top/2} A_{\theta}^{\top} G^{-1} A_{\theta} M^{1/2}) < \infty.$$

The following remark then establishes the strong convexity and Lipschitz smoothness of Φ_{θ}^M .

Remark 3.10. We note that

$$\|\nabla_z \Phi_{\theta}^M(z) - \nabla_z \Phi_{\theta}^M(z')\| \leq L_{\theta,M} \|z - z'\|,$$

where $L_{\theta,M} = \lambda_{\max}(M^{\top/2} A_{\theta}^{\top} G^{-1} A_{\theta} M^{1/2})$. Also note that Φ_{θ}^M is strongly convex with $m_{\theta,M} = \lambda_{\min}(M^{\top/2} A_{\theta}^{\top} G^{-1} A_{\theta} M^{1/2}) > 0$.

Proof. Assuming a valid preconditioning matrix (i.e. one that admits a square root $M = M^{1/2} M^{\top/2}$), then for any x we have

$$\begin{aligned} x^{\top} M^{1/2} A_{\theta}^{\top} G^{-1} A_{\theta} M^{\top/2} x &= \left(M^{\top/2} x \right)^{\top} A_{\theta}^{\top} G^{-1} A_{\theta} M^{\top/2} x \\ &= y^{\top} A_{\theta}^{\top} G^{-1} A_{\theta} y > 0 \end{aligned}$$

where $y = M^{\top/2} x$. Positivity is guaranteed as $A_{\theta}^{\top} G^{-1} A_{\theta}$ is positive definite. Thus $m_M > 0$ as $\lambda_{\min}(A_{\theta}^{\top} G^{-1} A_{\theta}) > 0$ for any θ . ■

We define

$$m_M = \inf_{\theta} m_{\theta,M} < \infty \quad \text{and} \quad L_M = \sup_{\theta} L_{\theta,M} < \infty.$$

We also define the worst-case condition number as in (3.2) for the preconditioned case as

$$(3.14) \quad \kappa_{\max}^M = \frac{L_M}{m_M},$$

and note that $\kappa_{\max}^M < \infty$ as a corollary of Lemma 3.9. Then, we can obtain the following bound.

Theorem 3.11. *Assume $0 < \eta \leq \frac{m_M}{4L_M^2}$. Then,*

$$\text{KL}(p_k(u) || p(u)) \leq e^{-m_M \eta^k} \mathbb{E} [\text{KL}(p_0(u), p(u|\theta))] + 8\eta d L_M \kappa_{\max}^M,$$

where L_M and κ_{\max}^M are defined in Lemma 3.9 and Eq. (3.14) respectively.

Proof. Considering Eq. (3.11), we consider the ULA for this diffusion as in the previous sections. This diffusion will converge to the measure $p(z|\theta)$, hence we obtain

$$\text{KL}(p_k(z|\theta) || p(z|\theta)) \leq e^{-m_{\theta,M} \eta^k} \text{KL}(p_0(z) || p(z|\theta)) + 8\eta d \frac{L_{\theta,M}^2}{m_{\theta,M}}.$$

Since the KL divergence is invariant under invertible transformations, we have

$$\text{KL}(p_k(M^{-1/2}u|\theta)||p(M^{-1/2}u|\theta)) = \text{KL}(p_k(u|\theta)||p(u|\theta)),$$

which implies that we can obtain the following bound

$$\text{KL}(p_k(u|\theta)||p(u|\theta)) \leq e^{-m_{\theta,M}\eta^k} \text{KL}(p_0(u)||p(u|\theta)) + 8\eta d \frac{L_{\theta,M}^2}{m_{\theta,M}}.$$

Then, it is straightforward to arrive at the result by taking expectations and using the chain rule of KL-divergence. \blacksquare

Remark 3.12. Theorem 3.11 shows that if one chooses a matrix M such that

$$\kappa_{\max}^M \ll \kappa_{\max},$$

then a significant improvement can be made in terms of error guarantees. Also note that the step-size condition in Theorem 3.11 (and similarly in other theorems) can be written as

$$0 < \eta \leq \frac{1}{4\kappa_{\max}^M L},$$

replacing the condition $0 < \eta \leq \frac{1}{4\kappa_{\max} L}$ appears in Theorem 3.3. This means that, if $\kappa_{\max}^M \ll \kappa_{\max}$, one can choose much larger step-sizes under the preconditioned case. This is what we precisely observe in the experimental section below.

Theorem 3.11 straightforwardly extends to the posterior case, i.e., for the sampler defined in (2.16)–(2.17). Similar to the case of the prior, we note the following lemma.

Lemma 3.13. *There exists $m_M^y > 0$ and $L_M^y > 0$ such that*

$$(3.15) \quad 0 < m_M^y = \inf_{\theta} \lambda_{\min}(M^{\top/2} \nabla^2 \Phi_{\theta}^y M^{1/2})$$

and

$$(3.16) \quad L_M^y = \sup_{\theta} \lambda_{\max}(M^{\top/2} \nabla^2 \Phi_{\theta}^y M^{1/2}) < \infty.$$

Proof. The proof is similar to the proof of Lemma 3.9 since the Hessian $\nabla^2 \Phi_{\theta}^y$ is positive definite by Assumption 2. \blacksquare

We define the worst-case condition number for the posterior case

$$(3.17) \quad \kappa_{\max}^{M,y} = \frac{L_M^y}{m_M^y}.$$

The convergence result then follows in the identical way as we have derived for the prior. In other words, we consider the diffusion

$$du_t = -M \nabla \Phi_{\theta}^y(u_t) dt + \sqrt{2} M^{1/2} dB_t,$$

and proceed in the same way as in the prior, which we omit due to space concerns. We summarise the final result of our paper as follows.

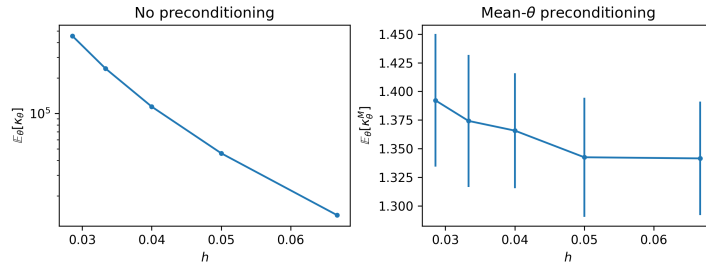
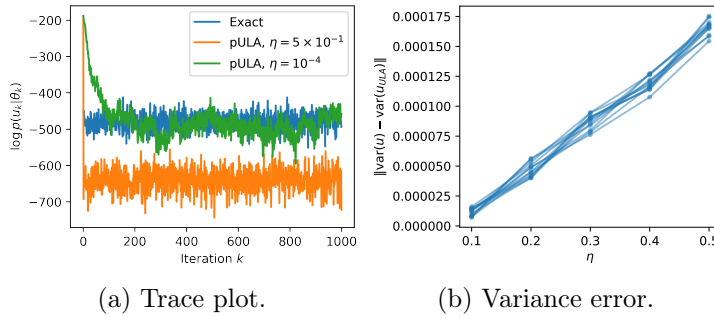


Figure 1: Expected condition number $\mathbb{E}_\theta[\kappa_\theta]$ of the precision $A_\theta^\top G^{-1} A_\theta$ (left), and expected condition number $\mathbb{E}_\theta[\kappa_\theta^M]$ of the preconditioned precision $M_\theta^{1/2} A_\theta^\top G^{-1} A_\theta M_\theta^{1/2}$ (right), for eight levels of mesh-refinement. Shown also are the estimated 50% probability intervals.



(a) Trace plot.

(b) Variance error.

Figure 2: Prior: results for state dimension $d = 1089$, plotting the sampled values of the log-target (a), and the errors on the variance, for 10 chains (b). For ULA, the stepsize offers a tradeoff between bias and rate of convergence: samplers that converge rapidly have a higher bias, which appears to increase linearly in η .

Theorem 3.14. *Assume that Assumption 2 holds and $0 < \eta \leq \frac{m_M^y}{4L_M^y/2}$. Then,*

$$\text{KL}(p_k(u|y)||p(u|y)) \leq e^{-m_M^y \eta k} \mathbb{E}[\text{KL}(p_0(u), p(u|\theta, y))] + 8\eta d L_M^y \kappa_{\max}^{M,y},$$

where L_M^y and κ_{\max}^M are defined in Lemma 3.13 and Eq. (3.17) respectively.

Proof. The proof is identical to the proof of Theorem 3.2, adapting the arguments for the prior to the posterior. ■

4. Empirical results. In this section we illustrate the ULA methodology, both with and without preconditioning, to sample from the prior and posterior measures. These results illustrate that ULA performs comparably, in terms of mean and variance estimates, to the standard Metropolis-adjusted algorithms. Preconditioning is seen to improve convergence, and allows for larger stepsizes. The effect of simulation parameters is also studied, quantifying the tradeoff between ULA bias, and rapidity of convergence. All implementations are contained

in an open-source Python package, available from <https://www.github.com/connor-duffin/ula-statfem>. We use Fenics [24] for all finite element discretisations.

4.1. Sampling the prior. We consider the Poisson problem

$$\begin{aligned} -\nabla \cdot (\theta(x)\nabla u(x)) &= f(x) + \xi(x), & x \in \Omega \\ u &= 0, & x \in \partial\Omega \end{aligned}$$

where $\Omega = [0, 1] \times [0, 1]$ and $f(x) \equiv 1$. Both θ and ξ are GPs, taking

$$\begin{aligned} \xi(x) &\sim \mathcal{GP}(0, 0.05^2 \delta(x - x')), \\ \log \theta(x) &\sim \mathcal{GP}(\log(1 + 0.3 \sin(\pi(x_0 + x_1))), k_{\text{se}}(x, x')), \quad k_{\text{se}} = 0.1^2 \exp\left(-\frac{\|x - x'\|^2}{2 \cdot 0.2^2}\right). \end{aligned}$$

Discretisation gives the conditional Gaussian $p(u|\theta) = \mathcal{N}(A_\theta^{-1}b, A_\theta^{-1}GA_\theta^{-\top})$, which can be marginalised over θ to give the prior $p(u) = \int p(u|\theta)p(\theta) d\theta$. We construct G by noting that

$$\begin{aligned} \tilde{G}_{ij} &= \beta^2 \int_{\Omega} \phi_i(x) \int \delta(x - x') \phi_j(x') dx' dx \\ &= \beta^2 \int_{\Omega} \phi_i(x) \phi_j(x) dx dx = \beta^2 M_{ij}, \end{aligned}$$

for the mass matrix M . A lumped approximation is made, to give the diagonal $G_{ii} = \sum_j \tilde{G}_{ij}$.

We compare the available Langevin methods to sample from the marginal $p(u)$, both with and without preconditioning. These are the Metropolis-adjusted Langevin algorithm (MALA), preconditioned MALA (pMALA), ULA, and preconditioned ULA (pULA). For preconditioning, the pMALA sampler uses the exact Hessian $M = A_{\theta_k}^{-1}GA_{\theta_k}^{-\top}$, and the pULA sampler uses the Hessian matrix with θ set to $\theta(x) = \bar{\theta}$, so $M = A_{\bar{\theta}}^{-1}GA_{\bar{\theta}}^{-\top}$ (from here on in, this is referred to as the mean- θ -Hessian). Figure 1 shows the effect of this preconditioner on the prior covariance matrix, under mesh-refinement, using standard MC sampling. We see that $\mathbb{E}_\theta[\kappa_\theta^M]$ is approximately six orders of magnitude smaller than $\mathbb{E}_\theta[\kappa_\theta]$, being near unity at various mesh-refinement levels. As the following examples will show, this preconditioner is very effective; in its absence the ULA sampler may diverge due to instability, and MALA mixes poorly.

We first compare the results of running two pULA samplers on a low-dimensional problem ($d = 1089$, triangular mesh with 32×32 cells), targeting $p(u)$. Each sampler has a ‘‘cold-start’’, setting $u_0 = 0$, and stepsizes are $\eta = 10^{-4}$ and $\eta = 5 \times 10^{-1}$. These results are shown in Figure 2, alongside samples from the exact measure. With a higher stepsize the bias inherent in the ULA method can be seen, which is traded for a faster converging sampler (Figure 2a). Variance errors are shown in Figure 2b, from running 5 pULA samplers for 10 chains each, with stepsizes increased from $\eta = 0.1$ up to $\eta = 0.5$. The error in the variance increases approximately linearly as we increase the stepsize; for faster convergence, we trade off more bias in the sampler.

Next, we increase the dimensionality, targeting $p(u)$ defined from the stochastic Poisson problem with dimension $d = 16,641$ (FEM mesh with 128×128 cells). For each sampler we run a single chain with 5000 warmup samples, and $K = 10,000$ post-warmup samples. For

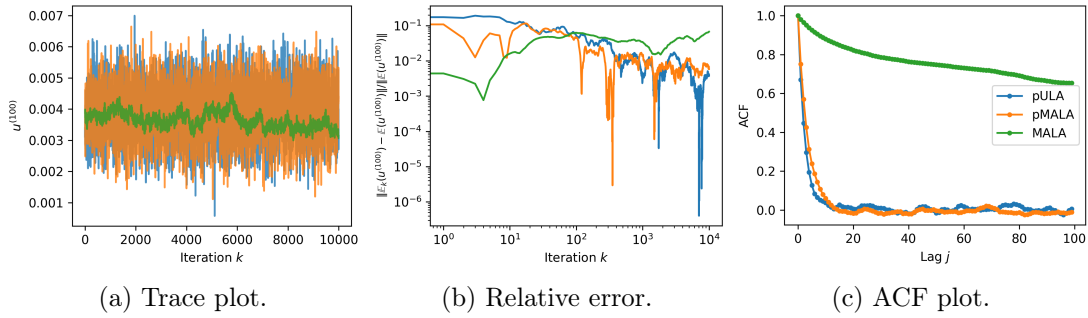


Figure 3: Prior: results for state dimension $d = 16,649$. Shown are the results for the finite element coefficient $u^{(100)}$, using the post-warmup samples. Preconditioning is essential for this problem, to avoid poor mixing.

the pULA sampler, each sample uses $n_{\text{inner}} = 10$ inner iterations. All samplers are initialised with an exact sample $u_0 \sim p(u)$; the warmup ensures that adequate stepsizes are chosen. The MALA samplers were each run with an adaptive stepsize during the warmup phase of the run, which increased or decreased η depending on the acceptance ratio, to ensure acceptance rates of $\approx 50\%$. This gives the highly restrictive stepsize $\eta \approx 2.5 \times 10^{-10}$ for MALA, and $\eta \approx 6 \times 10^{-2}$ for pMALA. For pULA, we use the dimensional stepsize of $d^{-1/3}$ [30] which is $\eta \approx 3.9 \times 10^{-2}$. For a variety of stepsizes the ULA scheme diverges due to numerical instability, typically failing in < 10 iterations.[‡] For this reason we do not show results for ULA, in this subsection.

Trace plots for the single FEM coefficient $u^{(100)}$ are shown in Figure 3a (other FEM coefficients give visually similar plots), and demonstrate appropriate mixing. In this case the exact-Hessian and the mean- θ -Hessian appear to give equivalent results (c.f. Table 1). The MALA sampler fails to explore the space due to the poor conditioning of $A_\theta^{-1}GA_\theta^{-\top}$. Figure 3b shows $\frac{\|\mathbb{E}_k(u^{(100)}) - \mathbb{E}(u^{(100)})\|}{\|\mathbb{E}(u^{(100)})\|}$, where $\mathbb{E}_k(u^{(100)}) = \frac{1}{k} \sum_{i=1}^k u_i^{(100)}$. The reference $\mathbb{E}(u^{(100)})$ is computed from 10,000 exact samples from $p(u)$. The convergence rates of the pULA and pMALA are visually equivalent, and the MALA sampler records no decrease in the error. The autocorrelation functions (ACFs), for the FEM coefficient $u^{(100)}$, are shown in Figure 3c, and accord with the previous results. The pULA and pMALA samplers give similar performance, and the MALA samples appear highly correlated.

Next we check the accuracy of the mean and the variance estimates with the relative errors of each, $\frac{\|\mathbb{E}_K(u) - \mathbb{E}(u)\|}{\|\mathbb{E}(u)\|}$, $\frac{\|\text{var}_K(u) - \text{var}(u)\|}{\|\text{var}(u)\|}$, computed against estimates from the exact reference samples. These are displayed in Table 1, and show that all samplers are accurate to order $O(10^{-2})$ in the mean. In the variance, the pULA sampler is more accurate than the pMALA, and the MALA gives a poor estimate. Note also that this provides no indication that the effects of the ULA bias are practically realised for this example, with pULA having smaller relative errors than the unbiased samples from pMALA. In terms of sampler

[‡]This is unsurprising given the poor condition number of the covariance matrix, when considered with Theorem 3.3.

Sampler	Error($\mathbb{E}(u)$)	Error($\text{var}(u)$)	ESS / s
pULA	0.004505	0.038913	4.605
pMALA	0.006356	0.060541	0.745
MALA	0.049279	0.994318	0.019

Table 1: Prior: relative norm errors of the mean and variance for each sampling method (errors are computed against the exact samples), for the 128×128 mesh. The ESS is computed from samples of the FEM coefficient $u^{(100)}$.

efficiency, as measured by the effective sample size per second (computed from the samples of the FEM coefficient $u^{(100)}$), preconditioning results in one and two orders of magnitude improvement over no preconditioning, for the pMALA and pULA samplers, respectively.

4.2. Sampling the posterior. We now detail the results for sampling the posterior $p(u | y)$, using the prior of the previous section $p(u | \theta) = \mathcal{N}(A_\theta^{-1}b, A_\theta^{-1}GA_\theta^{-\top})$. In this experiment we assume n_{obs} measurements are obtained at d_y locations. Denoting by $y_i \in \mathbb{R}^{d_y}$, gives the full dataset as $y = [y_1, \dots, y_{n_{\text{obs}}}] \in \mathbb{R}^{d_y \times n_{\text{obs}}}$. The observation process is $y_i = Hu + e$, $e \sim \mathcal{N}(0, R)$, and the likelihood is $p(y | u) = \prod_{i=1}^{n_{\text{obs}}} p(y_i | u)$, for $p(y_i | u) = \mathcal{N}(Hu, R)$.

Each observation vector is generated from an exact sample from the marginal $u^i \sim p(u)$, interpolated at the observation locations. To induce some sort of model mismatch, we scale this sample by a known scale factor, and then add on noise $e^i \sim p(e) = \mathcal{N}(0, R)$. We repeat this n_{obs} times to give the full dataset $y = [y_1, \dots, y_{n_{\text{obs}}}]$.

The conditional posterior $p(u | y, \theta)$ can be written out as

$$\begin{aligned}
 p(u | \theta, y) &= \mathcal{N}(m_{u,\theta}, C_{u,\theta}), \\
 m_{u,\theta} &= C_{u,\theta} \left(A_\theta^\top GA_\theta u + \sum_{i=1}^{n_{\text{obs}}} H^\top R^{-1} y_i \right), \\
 C_{u,\theta}^{-1} &= A_\theta^\top GA_\theta + n_{\text{obs}} H^\top R^{-1} H.
 \end{aligned}$$

We compute the marginal posterior $p(u | y) = \int p(u | y, \theta) p(\theta) d\theta$ with MALA, pMALA, ULA, pULA, and pCN. Based on results in the previous section, the preconditioned Langevin samplers (pULA and pMALA), employ the mean- θ -Hessian preconditioner, with $M^{-1} = A_\theta^\top G^{-1} A_\theta + H^\top R^{-1} H$. The proposal covariance matrix for pCN is the prior covariance. Full details are contained in the appendix.

In this section, the state dimension is the same as previous, with $d = 16,649$. We generate $n_{\text{obs}} = 100$ measurements of vectors of size $d_y = 128$ to give the data y . For each of the Metropolis-based methods, we generate 10,000 samples as warmup for each sampler, and $K = 10,000$ post-warmup samples. For the ULA samplers, we generate $K = 10,000$ samples using 10 inner iterations for each sample. All samplers are initialised to a sample from the exact posterior, $u_0 \sim p(u | y)$. During the warmup iterations, the adjusted MCMC algorithms MALA, pMALA, and pCN run an adaptive stepsize algorithm which automatically tunes the stepsize to give acceptance rates of approximately 50%. For the ULA sampler, we used $\eta = 1 \times 10^{-9}$, and for the pULA sampler we used the stepsize $\eta = d^{-1/3} \approx 3.9 \times 10^{-2}$.

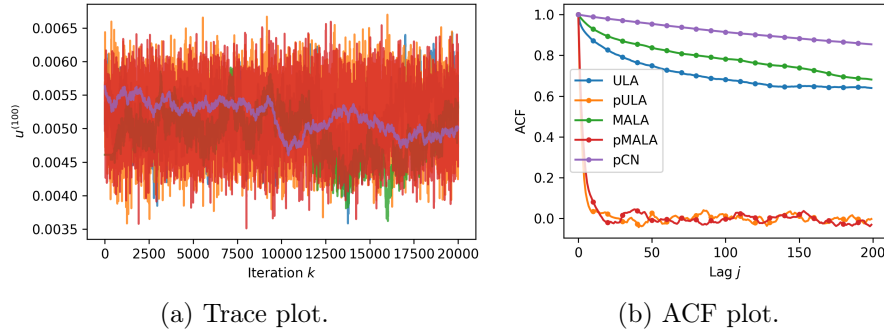


Figure 4: Linear posterior: results for state dimension $d = 16,649$; trace plots and ACF plots are shown for the FEM coefficient $u^{(100)}$. Compared to the standard pCN, the Langevin algorithms converge rapidly, with better UQ.

Sampler	Error($\mathbb{E}(u)$)	Error($\text{var}(u)$)	ESS / s
ULA	0.005508	0.546592	0.022
pULA	0.000234	0.025406	3.204
MALA	0.008382	0.785986	0.029
pMALA	0.000257	0.029731	1.52
pCN	0.00814	0.817542	0.012

Table 2: Linear posterior: relative norm errors of the mean and variance, for each sampling method, and the ESS per second, for the post-warmup samples. The errors are computed against 10^4 exact samples. The ESS/s is computed from the FEM coefficient $u^{(100)}$.

Trace plots for $u^{(100)}$ are shown in Figure 4a and demonstrate that all samplers converge to the target measure, with the pCN sampler giving notably poor mixing. This is also seen in the ACF (Figure 4b), where pCN exhibits the highest correlation correlated samples. For the non-preconditioned Langevin algorithms, adding in the MH correction results in increased correlations. For the preconditioned Langevin samplers, performance is comparable.

Table 2 shows the empirical results. The pCN, ULA, and MALA perform similarly to one another: each is accurate in the mean, but is inaccurate for the variance. Poor conditioning again makes the non-preconditioned Langevin samplers mix poorly, and the pCN struggles due to the prior covariance not capturing the posterior covariance structure. Preconditioned Langevin samplers are more performant, with both pMALA and pULA giving accurate estimates of the mean and variance, with two orders of magnitude improvement in the sampler efficiencies over pCN. The pULA sampler is approximately twice as efficient to the pMALA sampler. This is thought to be due to pULA taking larger stepsizes, for which the increase in bias is not realised in Table 2 (errors on the variance are similar for smaller for pULA vs. pMALA).

4.3. Sampling the nonlinear posterior. Finally, we detail the results for sampling the nonlinear posterior $p(u|y)$. In this case the data is generated from a nonlinear mapping of

the FEM coefficients, so that $y_i = \mathcal{H}(u) + e$, $e \sim \mathcal{N}(0, R)$, for $i = 1, \dots, n_{\text{obs}}$. In this case, $\mathcal{H} : \mathbb{R}^d \rightarrow \mathbb{R}^{n_y}$, and we assume that $\mathcal{H}(\cdot)$ is at least once differentiable. Data is simulated using the same procedure of the previous subsection, except that where solutions are interpolated with the observation operator H , we now use the nonlinear $\mathcal{H}(\cdot)$. In this case, we use a sigmoid function, defining

$$\mathcal{H}(u)_j = S((Hu)_j), \quad \text{with } S(x) = \frac{0.1}{1 + e^{-100(x-0.05)}},$$

which has the interpretation that past input values of ≈ 0.1 , the synthetic observation sensor saturates and is unable to distinguish between input values.

The prior of the previous subsection is used, $p(u | \theta) = \mathcal{N}(A_\theta^{-1}b, A_\theta^{-1}GA_\theta^{-\top})$, so, up to an additive constant, the potential is

$$\Phi_\theta^y(u) = \frac{1}{2} \sum_{i=1}^{n_{\text{obs}}} (y_i - \mathcal{H}(u))^\top R^{-1} (y_i - \mathcal{H}(u)) + \frac{1}{2} (A_\theta u - b)^\top G^{-1} (A_\theta u - b).$$

In this case no exact sampler is available so we use the same samplers of the previous section (ULA, MALA, pULA, pMALA, and pCN). For the preconditioned Langevin methods, the preconditioner M uses the inverse Gauss-Newton Hessian [6] defined at the maximum-a-posteriori (MAP) [27] estimate $u_* = \operatorname{argmin}_{u \in \mathbb{R}^d} \Phi_\theta^y(u)$. Letting $\mathcal{J}(u) = \nabla_u \mathcal{H}(u)$, this gives $M_\theta^{-1} = A_\theta^\top G^{-1} A_\theta + \mathcal{J}(u_*)^\top R^{-1} \mathcal{J}(u_*)$. In practice we also set $\theta = \bar{\theta}$, so that $M^{-1} = M_{\bar{\theta}}^{-1}$.

The experimental setup uses $n_{\text{obs}} = 100$ observations at $d_y = 128$ locations across the mesh, so $y \in \mathbb{R}^{d_y \times n_{\text{obs}}}$. Samplers are each initialised to the MAP estimate, $u_0 = u_*$, and are run for 2×10^4 warmup iterations and $K = 2 \times 10^4$ sampling iterations. Stepsizes are the same as previous. All samplers set $n_{\text{inner}} = 10$, apart from ULA, for which we set $n_{\text{inner}} = 50$ (this was found to improve sampler performance with a mild increase in runtime). The proposal covariance for pCN is again set to the prior covariance matrix.

Results are shown in Figure 5. All posterior means show agreement (Figure 5a), as do the variance fields for pULA and pMALA — the other samplers struggle to provide accurate UQ (c.f. Table 3). The ACF, which is shown in Figure 5b, suggests that correlations between samples are similar to the linear posterior (c.f. Figure 4b), with similar stratification of samplers. The Gauss-Newton Hessian, in this case, is able to provide a sensible preconditioner that increases mixing, giving a similar effect to that of the exact Hessian in the linear case. Table 3 quantifies sampler performance, and gives mostly similar results to the linear case. In this case MALA performs noticeably worse due to the poorer conditioning of the nonlinear problem. ULA is able to counteract this by taking larger stepsizes, whereas MALA remains constrained to ensure optimal acceptance rates.

5. Conclusions. We have provided an iterative sampling approach for constructing finite element solutions to stochastic PDEs. Our approach is in the same vein as iterative FEM solvers and targets scenarios where a direct sampling approach might not be feasible. Furthermore, leveraging the standard tools of Bayesian inference, we have provided a principled way to incorporate data the statistical finite element model. This construction blends the data assimilation and the model construction, paving the way of customising these constructions for

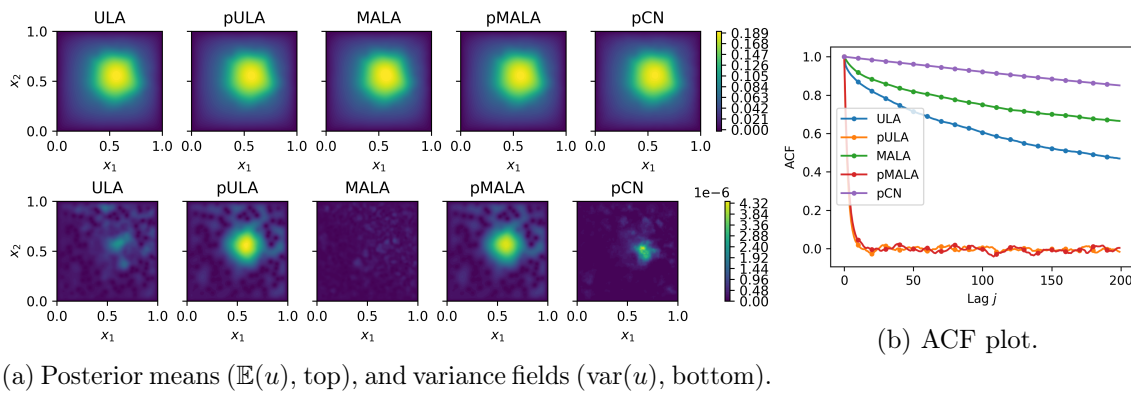


Figure 5: Nonlinear likelihood: posterior results. The ACF plot is shown for the samples from the FEM coefficient $u^{(100)}$. All samplers are accurate in the mean, but preconditioning captures the variance.

Sampler	Error($\mathbb{E}(u)$)	Error($\text{var}(u)$)	ESS / s
ULA	0.004063	0.615644	0.0228
pULA	0.000416	0.050948	3.2322
MALA	0.009769	0.898006	0.002
pMALA	0.000201	0.014455	1.3233
pCN	0.007586	0.760288	0.0091

Table 3: Nonlinear likelihood: relative norm errors of the mean and variance for each sampling method (errors are computed against 2×10^5 post-warmup pMALA samples), and the ESS is computed from the FEM coefficient $u^{(100)}$.

specific applications. The Langevin-based inference schemes we provide are generic as long as the gradients of the log-posteriors are available. Our future work plans include extending this framework to nonlinear PDEs using the results available for ULA for non-convex potentials [37, 1, 25] and use well-studied probabilistic tools within this framework, e.g., model selection.

Acknowledgements. We thank Valentin De Bortoli for useful discussions.

REFERENCES

- [1] Ö. D. AKYILDIZ AND S. SABANIS, *Nonasymptotic analysis of Stochastic Gradient Hamiltonian Monte Carlo under local conditions for nonconvex optimization*, arXiv preprint arXiv:2002.05465, (2020).
- [2] H. ALRACHID, L. MONES, AND C. ORTNER, *Some remarks on preconditioning molecular dynamics*, The SMAI journal of computational mathematics, 4 (2018), pp. 57–80.
- [3] J. O. BERGER AND L. A. SMITH, *On the Statistical Formalism of Uncertainty Quantification*, Annual Review of Statistics and Its Application, 6 (2019), pp. 433–460, <https://doi.org/10.1146/annurev-statistics-030718-105232>.
- [4] A. BESKOS, M. GIROLAMI, S. LAN, P. E. FARRELL, AND A. M. STUART, *Geometric MCMC for*

- infinite-dimensional inverse problems*, Journal of Computational Physics, 335 (2017), pp. 327–351, <https://doi.org/10.1016/j.jcp.2016.12.041>.
- [5] J. BRADBURY, R. FROSTIG, P. HAWKINS, M. J. JOHNSON, C. LEARY, D. MACLAURIN, G. NEČULA, A. PASZKE, J. VANDERPLAS, S. WANDERMAN-MILNE, AND Q. ZHANG, *JAX: composable transformations of Python+NumPy programs*, 2018, <http://github.com/google/jax>.
- [6] P. CHEN, *Hessian Matrix Vs. Gauss–Newton Hessian Matrix*, SIAM Journal on Numerical Analysis, 49 (2011), pp. 1417–1435.
- [7] Y. CHEN, T. A. DAVIS, W. W. HAGER, AND S. RAJAMANICKAM, *Algorithm 887: CHOLMOD, Supernodal Sparse Cholesky Factorization and Update/Downdate*, ACM Transactions on Mathematical Software, 35 (2008), pp. 22:1–22:14, <https://doi.org/10.1145/1391989.1391995>.
- [8] K. A. CLIFFE, M. B. GILES, R. SCHEICHL, AND A. L. TECKENTRUP, *Multilevel Monte Carlo methods and applications to elliptic PDEs with random coefficients*, Computing and Visualization in Science, 14 (2011), pp. 3–15, <https://doi.org/10.1007/s00791-011-0160-x>.
- [9] S. L. COTTER, G. O. ROBERTS, A. M. STUART, AND D. WHITE, *MCMC Methods for Functions: Modifying Old Algorithms to Make Them Faster*, Statistical Science, 28 (2013), pp. 424–446, <https://doi.org/10.1214/13-STS421>.
- [10] A. S. DALALYAN AND A. KARAGULYAN, *User-friendly guarantees for the Langevin Monte Carlo with inaccurate gradient*, Stochastic Processes and their Applications, 129 (2019), pp. 5278–5311.
- [11] C. R. DIETRICH AND G. N. NEWSAM, *Fast and Exact Simulation of Stationary Gaussian Processes through Circulant Embedding of the Covariance Matrix*, SIAM Journal on Scientific Computing, 18 (1997), pp. 1088–1107, <https://doi.org/10.1137/S1064827592240555>.
- [12] T. J. DODWELL, C. KETELSEN, R. SCHEICHL, AND A. L. TECKENTRUP, *A Hierarchical Multilevel Markov Chain Monte Carlo Algorithm with Applications to Uncertainty Quantification in Subsurface Flow*, arXiv:1303.7343 [math], (2015), <https://arxiv.org/abs/1303.7343>.
- [13] C. DUFFIN, E. CRIPPS, T. STEMLER, AND M. GIROLAMI, *Low-rank statistical finite elements for scalable model-data synthesis*, arXiv:2109.04757 [cs, math, stat], (2021), <https://arxiv.org/abs/2109.04757>.
- [14] C. DUFFIN, E. CRIPPS, T. STEMLER, AND M. GIROLAMI, *Statistical finite elements for misspecified models*, Proceedings of the National Academy of Sciences, 118 (2021).
- [15] A. DURMUS, E. MOULINES, ET AL., *Nonasymptotic convergence analysis for the unadjusted Langevin algorithm*, The Annals of Applied Probability, 27 (2017), pp. 1551–1587.
- [16] A. DURMUS, E. MOULINES, ET AL., *High-dimensional Bayesian inference via the unadjusted Langevin algorithm*, Bernoulli, 25 (2019), pp. 2854–2882.
- [17] E. FEBRIANTO, L. BUTLER, M. GIROLAMI, AND F. CIRAK, *A Self-Sensing Digital Twin of a Railway Bridge using the Statistical Finite Element Method*, arXiv:2103.13729 [cs, math], (2021), <https://arxiv.org/abs/2103.13729>.
- [18] M. B. GILES, *Multilevel Monte Carlo methods*, Acta Numerica, 24 (2015), pp. 259–328, <https://doi.org/10.1017/S096249291500001X>.
- [19] M. GIROLAMI AND B. CALDERHEAD, *Riemann Manifold Langevin and Hamiltonian Monte Carlo Methods*, Journal of the Royal Statistical Society: Series B (Statistical Methodology), 73 (2011), pp. 123–214, <https://doi.org/10.1111/j.1467-9868.2010.00765.x>.
- [20] M. GIROLAMI, E. FEBRIANTO, G. YIN, AND F. CIRAK, *The statistical finite element method (statFEM) for coherent synthesis of observation data and model predictions*, Computer Methods in Applied Mechanics and Engineering, 375 (2021), p. 113533.
- [21] I. G. GRAHAM, F. Y. KUO, D. NUYENS, R. SCHEICHL, AND I. H. SLOAN, *Quasi-Monte Carlo methods for elliptic PDEs with random coefficients and applications*, Journal of Computational Physics, 230 (2011), pp. 3668–3694, <https://doi.org/10.1016/j.jcp.2011.01.023>.
- [22] M. C. KENNEDY AND A. O’HAGAN, *Bayesian calibration of computer models*, Journal of the Royal Statistical Society: Series B (Statistical Methodology), 63 (2001), pp. 425–464, <https://doi.org/10.1111/1467-9868.00294>.
- [23] K. J. H. LAW, *Proposals which speed up function-space MCMC*, Journal of Computational and Applied Mathematics, 262 (2014), pp. 127–138, <https://doi.org/10.1016/j.cam.2013.07.026>.
- [24] A. LOGG, K.-A. MARDAL, AND G. WELLS, *Automated Solution of Differential Equations by the Finite Element Method: The FEniCS Book*, vol. 84, Springer Science & Business Media, 2012.
- [25] A. LOVAS, I. LYTRAS, M. RÁSONYI, AND S. SABANIS, *Taming neural networks with tusla: Non-convex*

- learning via adaptive stochastic gradient langevin algorithms*, arXiv preprint arXiv:2006.14514, (2020).
- [26] J. MARTIN, L. C. WILCOX, C. BURSTEDDE, AND O. GHATTAS, *A Stochastic Newton MCMC Method for Large-Scale Statistical Inverse Problems with Application to Seismic Inversion*, SIAM Journal on Scientific Computing, 34 (2012), pp. A1460–A1487, <https://doi.org/10.1137/110845598>.
- [27] K. P. MURPHY, *Machine Learning: A Probabilistic Perspective*, Adaptive Computation and Machine Learning Series, MIT Press, Cambridge, MA, 2012.
- [28] L. N. OLSON AND J. B. SCHRODER, *PyAMG: Algebraic multigrid solvers in Python v4.0*, 2018.
- [29] C. P. ROBERT AND G. CASELLA, *Monte Carlo statistical methods*, John Wiley & Sons, 2004.
- [30] G. O. ROBERTS AND J. S. ROSENTHAL, *Optimal scaling for various Metropolis-Hastings algorithms*, Statistical Science, 16 (2001), <https://doi.org/10.1214/ss/1015346320>.
- [31] Y. SAATCI, *Scalable Inference for Structured Gaussian Process Models*, PhD thesis, University of Cambridge, 2011.
- [32] A. M. STUART, *Inverse problems: A Bayesian perspective*, Acta Numerica, 19 (2010), pp. 451–559, <https://doi.org/10.1017/S0962492910000061>.
- [33] S. VEMPALA AND A. WIBISONO, *Rapid convergence of the unadjusted Langevin algorithm: Isoperimetry suffices*, Advances in neural information processing systems, 32 (2019), pp. 8094–8106.
- [34] J.-P. VIAL, *Strong and weak convexity of sets and functions*, Mathematics of Operations Research, 8 (1983), pp. 231–259.
- [35] C. VILLANI, *Optimal transport: old and new*, vol. 338, Springer, 2009.
- [36] A. WIBISONO, *Sampling as optimization in the space of measures: The Langevin dynamics as a composite optimization problem*, in Conference on Learning Theory, PMLR, 2018, pp. 2093–3027.
- [37] Y. ZHANG, Ö. D. AKYILDIZ, T. DAMOULAS, AND S. SABANIS, *Nonasymptotic estimates for Stochastic Gradient Langevin Dynamics under local conditions in nonconvex optimization*, arXiv preprint arXiv:1910.02008, (2019).

Appendices.

Appendix A. Lemmata.

Lemma A.1. (*The Chain Rule of the KL divergence*) Let $p(x_1, \dots, x_d)$ and $q(x_1, \dots, x_d)$ be two arbitrary probability distributions on \mathbb{R}^d . For $j \in \{1, \dots, d\}$, we denote the marginals of p and q on the first j coordinates by $p^{(j)}$ and $q^{(j)}$, i.e.,

$$p^{(j)} = \int \cdots \int p(x_1, \dots, x_d) dx_{j+1} \cdots dx_d,$$

and

$$q^{(j)} = \int \cdots \int q(x_1, \dots, x_d) dx_{j+1} \cdots dx_d.$$

Then

$$\text{KL}(p^{(1)}||q^{(1)}) \leq \text{KL}(p^{(2)}||q^{(2)}) \leq \cdots \leq \text{KL}(p||q),$$

i.e., the function $j \mapsto \text{KL}(p^{(j)}||q^{(j)})$ is increasing.

Lemma A.2. Let μ_θ and ν_θ be two conditional measures. Let μ and ν be their marginals, i.e.

$$\mu = \int \mu_\theta p(d\theta) \quad \text{and} \quad \nu = \int \nu_\theta p(d\theta).$$

Then, we have

$$(A.1) \quad W_2^2(\mu, \nu) \leq \mathbb{E}_\theta [W_2^2(\mu_\theta, \nu_\theta)].$$

Proof. Note that

$$\mathbb{E}_\theta [W_2^2(\mu_\theta, \nu_\theta)] = \int \inf_{\gamma_\theta \in \Gamma(\mu_\theta, \nu_\theta)} \int \|u - u'\|_{\gamma_\theta} p(du, du').$$

Now we take $\gamma_\theta^* \in \Gamma(\mu_\theta, \nu_\theta)$ that attains the infimum and write

$$\begin{aligned} \mathbb{E}_\theta [W_2^2(\mu_\theta, \nu_\theta)] &= \int \int \|u - u'\|_{\gamma_\theta^*} p(du, du'), \\ &= \int \|u - u'\|_{\gamma^*} p(du, du'), \\ &\geq W_2^2(\mu, \nu), \end{aligned}$$

where the second line follows from measurability of γ_θ^* (see [35, Corollary 5.22]). \blacksquare

Appendix B. Gaussian process on structured grids. To speed up sampling $\theta(x)$ we make use of the regular mesh [31]. In this work we use two-dimensional regular meshes for all simulations. The log-Gaussian process $\theta(x)$ can make use of this regular structure due to separability of $k_{\text{se}}(x, x')$ across spatial dimensions. We can write the n_m^2 nodes of the mesh Ω_h as a Cartesian product between two sets $\mathcal{X}_1 \times \mathcal{X}_2$, denoting the nodal locations as $\mathcal{X}_1 = (x_{1,1}, \dots, x_{1,n_m})$, $\mathcal{X}_2 = (x_{2,1}, \dots, x_{2,n_m})$. Then the GP covariance matrix K can be written as a Kronecker product, $K = K_1 \otimes K_2$, where $K_{1,ij} = k_{\text{se}}(x_{1,i}, x_{1,j})$, $K_{2,ij} = k_{\text{se}}(x_{2,i}, x_{2,j})$. The Cholesky decomposition $K = LL^\top$ can also be written as $LL^\top = (L_1 \otimes L_2)(L_1 \otimes L_2)^\top$, where $K_1 = L_1L_1^\top$, $K_2 = L_2L_2^\top$.

This means that the covariance matrix never needs to be stored in memory. Instead, the Kronecker factors K_1 and K_2 are stored, which gives reduction in memory (in terms of floating point numbers) from $\mathcal{O}((n_m^2)^2)$ to $\mathcal{O}(n_m^2)$. Also, we need only take the Cholesky on the n_m -dimensional nodal locations, which requires $\mathcal{O}(n_m^3/3)$ work, as opposed to the full 2D mesh, which would require $\mathcal{O}((n_m^2)^3/3)$ operations. Finally, making use of the ‘‘vec trick’’, we can perform matrix-vector multiplications with $L = (L_1 \otimes L_2)$ in $\mathcal{O}(n_m^2)$ time as opposed to $\mathcal{O}((n_m^2)^2)$.

Appendix C. Metropolis-adjusted Langevin algorithms. In this section we detail the Metropolis-adjusted Langevin samplers that we use in this paper. For more details see [19]. For a fixed θ , recall that the ULA proposal step (as in (2.9)), is given by

$$u_* = u_k - \eta \nabla \Phi_\theta(u_k) + \sqrt{2\eta} Z_{k+1},$$

which defines a proposal density for a Metropolis sampler, $q(u_* | u_k, \theta) = \mathcal{N}(u_* - \eta \nabla \Phi_\theta(u_k), 2\eta I)$. Preconditioning the proposal with a symmetric positive-definite matrix M gives the proposal density $q(u_* | u_k, \theta) = \mathcal{N}(u_* - \eta M \nabla \Phi_\theta(u_k), 2\eta M)$. The acceptance ratio for the prior is

$$\alpha(u_*; u_k, \theta) = \min \left\{ 1, \frac{p(u_* | \theta)}{p(u_k | \theta)} \cdot \frac{q(u_k | u_*, \theta)}{q(u_* | u_k, \theta)} \right\},$$

and is similarly defined for the posterior. This is computed on the log-scale to avoid underflow.

For the joint update of (u, θ) , we use a similar method to that proposed for ULA: for a sampled value $\theta_k \sim p(\theta)$, we run a MALA chain for a specified number of inner iterations n_{inner} , sampling $u_i^k \sim p(u | \theta_k)$, for $i = 1, \dots, n_{\text{inner}}$. The joint sample is then taken to be $(u_{n_{\text{inner}}}^k, \theta_k) \sim p(u, \theta)$.

Appendix D. Preconditioned-Crank Nicolson. We also compare the preconditioned-Crank Nicolson (pCN) sampler in the posterior case. The pCN sampler builds upon the idea that proposals which are reversible with respect to the *prior measure* only require computing a likelihood ratio for the acceptance probability. In the linear case we sample from a posterior $p(u | y, \theta)$ which can be written as

$$p(u | y, \theta) \propto \exp \left(-\frac{1}{2} (y - Hu)^\top R^{-1} (y - Hu) - \frac{1}{2} (u - A_\theta^{-1}b)^\top (A_\theta^{-1}GA_\theta^{-\top})^{-1} (u - A_\theta^{-1}b) \right).$$

Now, if we consider the pCN proposal, defined by

$$u_* = A_\theta^{-1}b + \sqrt{1 - \beta^2}(u_k - A_\theta^{-1}b) + \beta\tilde{Z}_k, \quad \tilde{Z}_k \sim \mathcal{N}(0, A_\theta^{-1}GA_\theta^{-\top}),$$

then by some algebra it can be shown that the acceptance probability is

$$\alpha(u_*, u_k; \theta) = \min \left\{ 1, \exp \left(-\frac{1}{2}(y - Hu_*)^\top R^{-1}(y - Hu_*) + \frac{1}{2}(y - Hu_k)^\top R^{-1}(y - Hu_k) \right) \right\},$$

i.e., a likelihood ratio. For the joint update of (u, θ) , again, we use a similar method to that proposed for ULA: for a sampled value $\theta_k \sim p(\theta)$, we run a pCN chain n_{inner} iterations, sampling $u_i^k \sim p(u | \theta_k)$, for $i = 1, \dots, n_{\text{inner}}$. The joint sample is then taken to be $(u_{n_{\text{inner}}}^k, \theta_k) \sim p(u, \theta)$.

Appendix E. Numerical details. We compute all samples using a workstation with an AMD Ryzen 9 5950X, with 128 GB memory. For the prior case, the exact sampler uses a smoothed aggregation Algebraic Multigrid (AMG) solver, accelerated with Conjugate Gradients, with 4 levels of coarseness to solve the linear system. This is implemented using the Python package `pyAMG` [28]. For the posterior case, the exact sampler uses the sparse Cholesky decomposition as implemented in `CHOLMOD` [7]. The nonlinear likelihood is implemented in `JAX` [5], and makes use of automatic differentiation when computing $\nabla_u \Phi_\theta^y(u)$. We also just-in-time compile (JIT) both the log-likelihood and the gradient.

For applying preconditioners, in both the prior and posterior case, again we use the sparse Cholesky decomposition (in this case the Hessian is sparse). For the mean- θ -Hessian preconditioners this is computed once and reused for the entire chain. For the exact-Hessian preconditioner we compute the symbolic factorization before running the chain, as the sparsity pattern of the Hessian does not change.